Electronic Supplementary Material (ESI) for Physical Chemistry Chemical Physics.
This journal is © the Owner Societies 2022

Supporting Information for Effect of an axial ligand on the self-assembly of molecular platforms

Chao Li,[†] Xiangzhi Meng,[†] Alexander Weismann,[†] Jan-Simon von Glasenapp,[‡] Feifei Xiang,[¶] Carlo A. Pignedoli,[¶] Rainer Herges,[‡] and Richard Berndt[*,†]

[†]*Institut für Experimentelle und Angewandte Physik, Christian-Albrechts-Universität zu Kiel, 24098 Kiel, Germany*

[‡]*Otto-Diels-Institut für Organische Chemie, Christian-Albrechts-Universität zu Kiel, 24098 Kiel, Germany*

[¶]*nanotech@surfaces Laboratory, EMPA, Swiss Federal Laboratories for Materials Science and Technology, 8600 Dübendorf, Switzerland*

E-mail: berndt@physik.uni-kiel.de

S.1 Instruments and measurements

Experiments were carried out in ultrahigh vacuum with a STM cooled to ≈ 4.6 K. The Ag(111) substrate was prepared by cycles of Ar^+ sputtering (1.5 keV) and annealing to 500 °C. Biphenyl-TOTA molecules were sublimated from a heated crucible (≈ 180 °C) onto the substrate at ≈ 25 °C. The deposition was followed by annealing at 80 °C for 5 minutes. STM tips were electrochemically etched from W wire and annealing *in vacuo*. STM imaging at constant current was performed at 4.6 K.

S.2 Calculations

DFT calculations of an isolated molecule and biphenyl-TOTA dimers on the Ag surface were performed using the CP2K code[1] by means of AiiDAlab apps[2] based on AiiDA.[3] We used the PBE parameterization of the exchange-correlation functional[4] together with the DFT-D3 van der Waals scheme proposed by Grimme[5] and norm-conserving GTH pseudopotentials.[6] A TZV2P MOLOPT basis set[7] was used for O, C, and H species and a DZVP MOLOPT basis set for the Ag atoms together with a cutoff of 600 Ry for the plane wave basis set. The surface/adsorbate systems were modeled within the repeated slab scheme. The biphenyl-TOTA molecule and the dimer were placed on four-layer 23.23×25.15 Å^2 and 40.65×30.18 Å^2 slabs of Ag(111) corresponding to 320 and 672 surface unit cells, respectively. A layer of hydrogen atoms was added at the bottom of Ag(111) slab to passivate the other side of the Ag slab to suppress the surface state. A vacuum layer of 48 Å thickness was added to decouple the system from its periodic replicas in the direction perpendicular to the surface. The adsorption geometry was optimized by keeping the positions of the two bottom Ag layers and the hydrogen layer fixed to the ideal bulk coordinates, while all other atoms were relaxed until forces were lower than 5 meV/Å. Scanning tunneling microscopy (STM) images were simulated within the Tersoff-Hamann approximation[8] using Kohn-Sham orbitals. The orbitals were extrapolated to the vacuum region to correct for the error induced by the localized basis set used.[9]

The calculations of gas-phase structures were carried on a revPBE[10]/def2-SVP[11] level of theory using ORCA.[12] The resolution of identity approximation (RI) was used in combination with the auxiliary basis set def2/J[13] and Grimme's D3 dispersion correction.[14]

S.3 Energy cost for tilting

We used a models of a biphenyl-TOTA dimer to calculate the bending angles of the biphenyl moieties and their total energy compared to the initial model. Figure S1 shows that the energy required to bend the biphenyl groups in a dimer configurations is less than 10 meV for bending angles smaller than 3°, and reaches ≈ 39 meV for a bending angle of 8°.

We also try to add the substrate for the calculations. To match the proposed STM image it was deemed necessary to fix the upper phenyl ring in a tilted position with respect to the Ag surface (see Figure S2, green phenyl subunit). Tilt angles of 0° and 8.7° were used to account for the minimum and maximum strain observed. Figure S2 (a) shows a schematic representation of the unstrained biphenyl-TOTA, while (b) shows a tilted and therefore strained structure.

To achieve the needed rotational and translational freedom while fixing the angle of the upper phenyl plane we constructed a system of dummy atoms in addition to the frozen Ag monolayer. (See Figure S3)

Angle constraints were imposed on X_1–X_4 to construct a plane parallel to the Ag surface, which retains a flexibility in the z-direction. Y_1–Y_3 were fixed to the X-plane but retain xy movement. To avoid a 180° bond angle the angle $\angle Y_1Y_2Y_3$ was not fixed directly. A fixed angle was rather achieved by introducing two dihedral angles which include one Z-atom, two Y-atoms and the C_4 atom of the upper phenyl instead. (For more detail see input below.) Z-atoms were fixed perpendicular to the X-plane below Y_1 and Y_2. A combination of a biphenyl-TOTA and the dummy system shown in Figure S4.

The imposed constraints lead to a translational freedom for the dummy system and the upper phenyl in the x, y and z directions within the limits of the Ag surface and allow for a

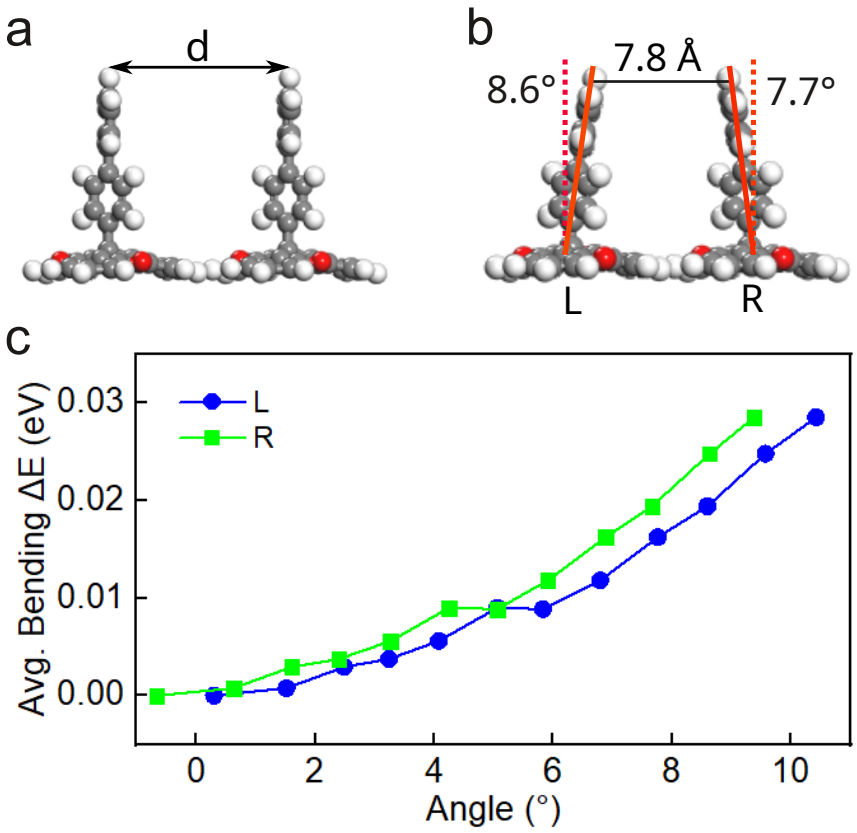

Figure S1: Bending angle of the biphenyl subunit in a biphenyl-TOTA dimer in gas phase. The initial configuration of the dimer was optimized on a four-layer Ag(111) slab, in which the two biphenyl groups are vertical to the corresponding TOTA platform with a distance of 1.06 nm. In this gas phase calculation, the Ag slab was then removed and the TOTA platforms were fixed during the relaxation. (a) The bending angles of the biphenyl groups in the biphenyl-TOTA dimer were tuned by changing the separation of the top H atoms. (b) The optimized dimer exhibits bending angles of 8.6° and 7.7°, which fits to the experimental values. (c) Evolution of the average energy as a function of the bending angle in each biphenyl group. The bending angle of each biphenyl group is defined as the angle of biphenyl with respect to the z-axis shown in (b) (dashed line). The energy of the initial configuration with the bending angle of 0.3 (L) and $-0.66°$ (R) is set to 0.

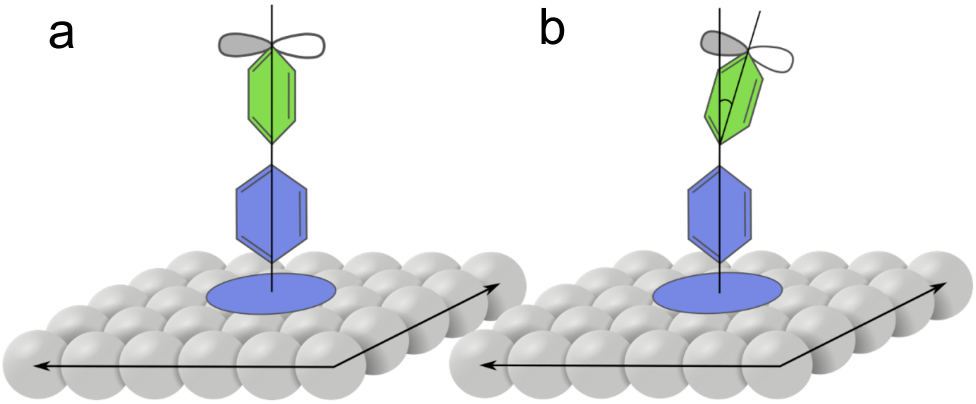

Figure S2: Schematic representation of a biphenyl-TOTA on a monolayer of Ag atoms. (a) Unstrained biphenyl-TOTA with a tilt angle of 0°. (b) Top phenyl plane tilted with respect to the Ag surface (p-orbital perpendicular to phenyl plane) imposing strain to the system. To achieve a set angle for the p-orbital at the top, the rotation around the C_1–C_4 axis of the upper phenyl must be suppressed.

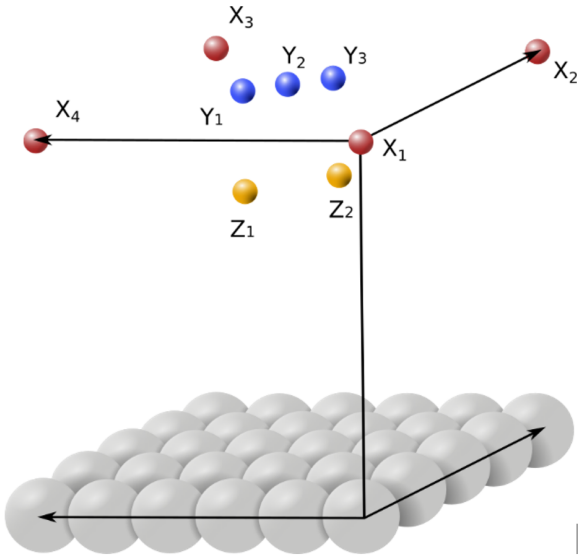

Figure S3: System of dummy atoms above the Ag monolayer. X_1–X_4 define a plane parallel to the Ag surface. Y_1–Y_3 were fixed to the X-plane. Z-atoms were fixed perpendicular to the X-plane below Y_1 and Y_2.

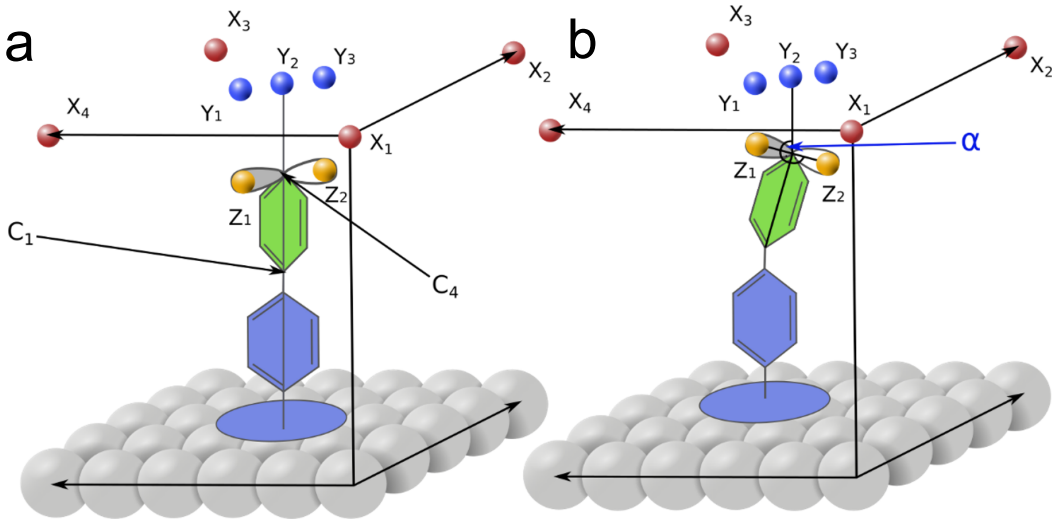

Figure S4: System of dummy atoms with a schematic representation of the biphenyl-TOTA. (a) For 0° tilt angle the angles $\angle C_1C_4Z_1$, $\angle Z_1C_4Y_2$, $\angle C_1C_4Z_2$ and $\angle Z_2C_4Y_2$ are fixed to 90°. (b) $\angle C_1C_4Z_1$ and $\angle C_1C_4Z_2$ are fixed to 90° while α ($\angle Z_1C_4Y_2$) was adjusted to 81.3° and $\angle Z_2C_4Y_2$ was fixed to 98.7°. To avoid rotation of the upper phenyl around the C_1–C_4 axis two dihedral angles ($Z_1C_4C_1C_2$ and $Z_2C_4C_1C_6$) were introduced.

precession around the Y_2C_4 axis as shown in Figure S5.

As expected for a system with many constraints the energy started to oscillate and the predefined angles exhibited minor variations. The optimization was stopped at this point and the dummy system as adjusted to match the specifications above once again, the angle of the upper phenyl was adjusted in the same way and the optimization was restarted. Several iterations of this procedure were necessary to achieve convergence. The energy to tilt one biphenyl-TOTA by 8.7° was calculated to be 1.32 kcal/mol (57 meV).

S.4 Phenyl-Phenyl interaction: Sandwich structure

To verify the method used and to quantify the phenyl-phenyl interaction we studied the interaction of two benzenes for different tilt angles. The scans were carried out as a set of single point calculations generated from an optimized benzene monomer with TmoleX 18.[15]

The distance scan for the benzene sandwich dimer yields a distinct minimum at 0.37 nm and a binding energy of −3.09 kcal/mol (134 meV). As expected for the small basis set the

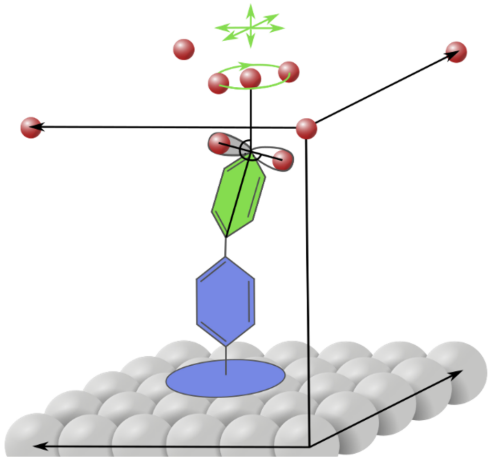

Figure S5: Schematic representation of the allowed translational and precession motions after imposing constraints to the system. The lower part of the molecule (blue) is not affected by the constraints except for the position of C_1.

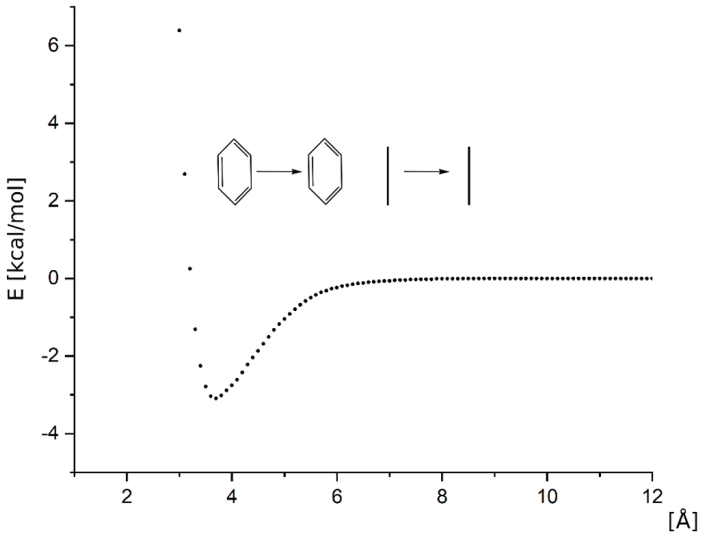

Figure S6: Distance scan for a benzene dimer in sandwich configuration.

minimum is slightly shifted to a smaller distance when compared to the QCISD(T)/aug-cc-pVTZ calculations by Janowski and Pulay (0.39 nm),[16] while the binding energy for revPBE/def2-SVP is nearly twice as high as the binding energy predicted by Janowski *et al.* (−1.65 kcal/mol = 72 meV).[15] The calculations show the expected behavior. Basis set superposition errors (BSSEs) are more prominent for smaller basis sets.[17–19] Unfortunately, using a larger basis set was not feasible for the calculations of the scale and quantity needed for this work.

S.5 Benzene-dimer 0°/8.7° tilt angle

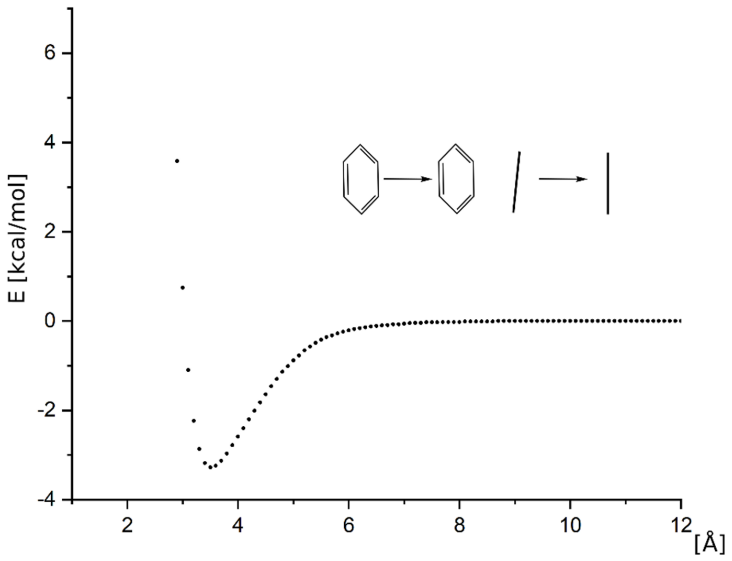

Figure S7: Distance scan for a benzene dimer in sandwich configuration with one of the benzenes tilted 8.7° toward the other. The scan shows a distinct energy minimum for a distance of 0.35 nm with a binding energy of −3.28 kcal/mol (142 meV). The distance is defined as the separation between the closest C-atoms of both rings.

S.6 Benzene-dimer 8.7°/8.7° tilt angle

Within the limit set by the scale of the needed calculations the method used provides a reasonable description of the benzene-benzene interaction. No or little interaction was observed for benzene distances exceeding 0.7 nm. Since only the top part of the biphenyl rotor is

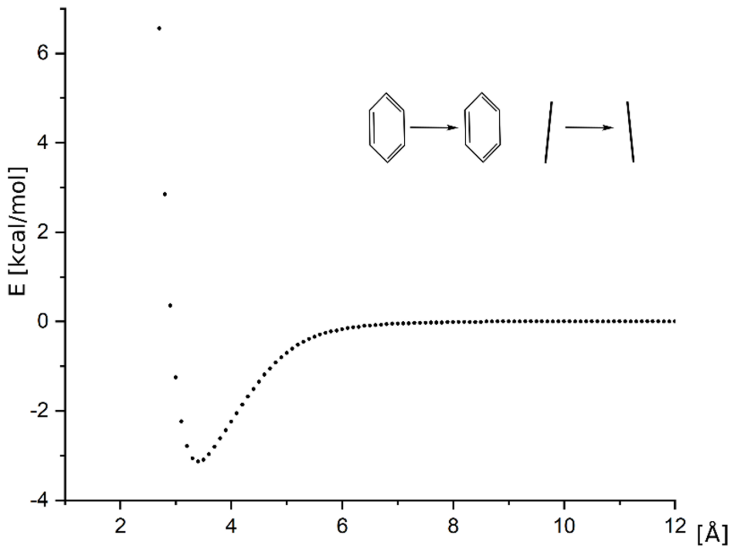

Figure S8: Distance scan for a benzene dimer in sandwich configuration with both benzenes tilted 8.7° toward each other. The scan shows a distinct energy minimum for a distance of 0.34 nm with a binding energy of −3.13 kcal/mol (136 meV). The distance is defined as the distance between the closest C-atoms of both rings.

observed in the STM image we decided to build a system based only on the proposed tilt of the upmost p-orbital.

S.7 Position of the Phenylspacer

Rotational scans of a TOTA dimer with one phenyl rotor were performed for a center-to-center distances of 1.04 and 0.94 nm. We performed four 30° scan for each center-to-center distance to cover 120° for θ (see Figures S9).

The phenyl position with one hydrogen above the TOTA oxygen that interacts with a hydrogen of the second TOTA platform (0° in Figures S9) is preferred by 0.44 – 0.46 kcal/mol (19 – 20 meV) for 0.94 nm and 0.08 – 0.125 kcal/mol (3 – 5 meV) for 1.04 nm.

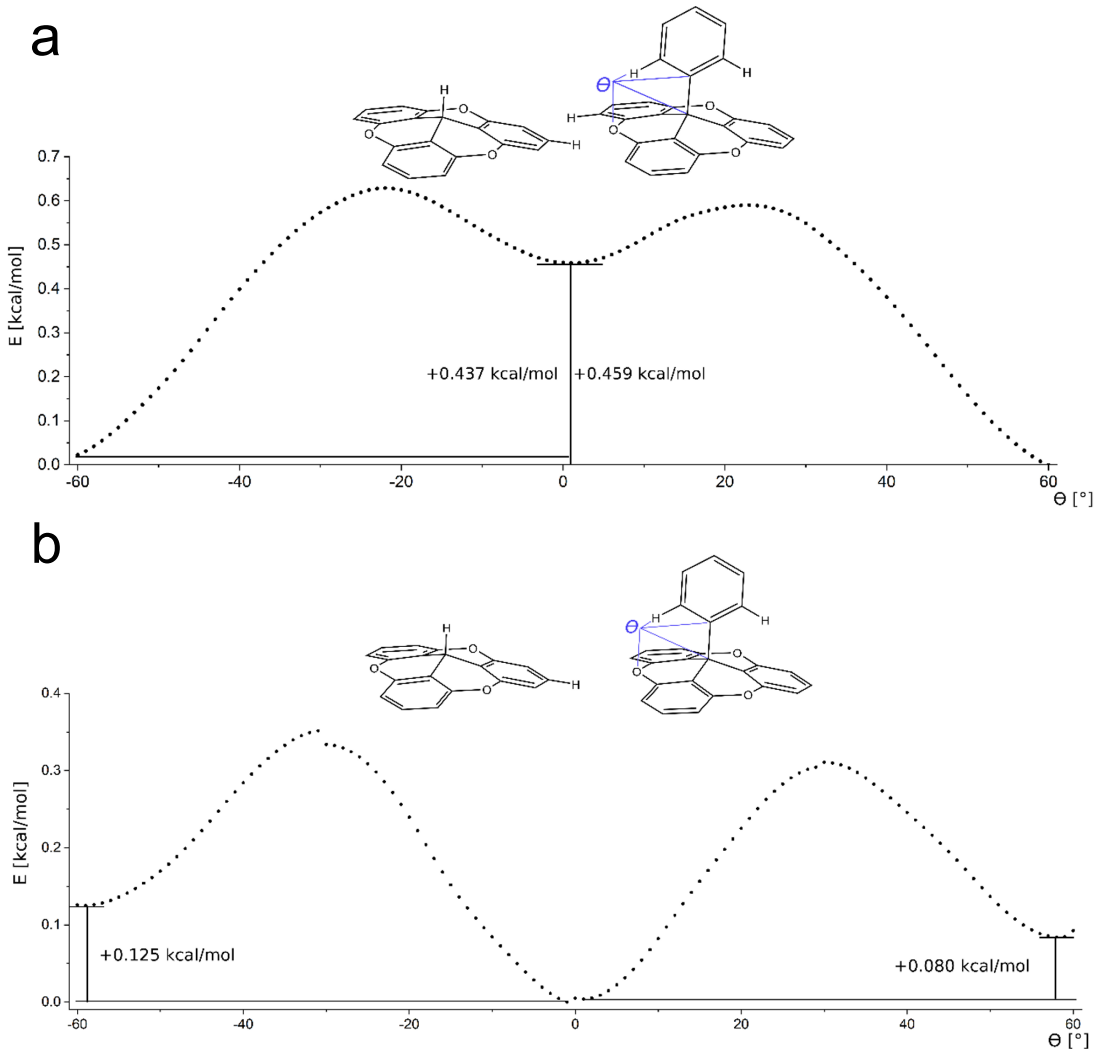

Figure S9: (a) Rotational scan of θ for a Phenyl TOTA and a hydrogen TOTA in head (triangle vertex in TOTA platform) to side (triangle side in TOTA platform) configuration, with a center-to-center distance of 0.94 nm, composed of four 30° scans. The position of a phenyl hydrogen above the already bonded oxygen is favored by 0.44–0.46 kcal/mol (19 – 20 meV). The energy range (1 meV) reflects the error in the SCF energy for the different 30° scans. (b) Rotational scan of θ for a Phenyl and a hydrogen TOTA in head to side configuration, with a center-to-center distance of 1.04 nm, composed of four 30° scans. The position of a phenyl hydrogen above the already bonded oxygen is favored by 0.08–0.125 kcal/mol.

S.8 Synthesis

4-Trimethylstannyl-1,1'-biphenyl (Fig. S10) Under a nitrogen atmosphere, 4-Iodo-1,1'-biphenyl (712 mg, 2.54 mmol), hexamethyl-distannane (1.00 g, 3.05 mmol, 1.2 eq.) and tetrakis(triphenylphosphine)-palladium(0) (58.7 mg, 50.8 µmol, 2 mol%) were suspended in dry toluene (5 mL) and anhydrous 2-methyltetrahydrofurane (0.3 mL) in a microwave vial. The mixture was stirred and heated in a microwave reactor at 150 °C and 200 W for 10 min. Subsequently, the mixture was filtered over celite, the solvents evaporated and the crude product subjected to column chromatography (stationary phase: silica gel, eluent: cyclohexane/ethyl acetate (4:1, Rf = 0.19) to afford the pure product as a colourless oil, which solidifies upon cooling (492 mg, 1.55 mmol, 61 %). Analytical data were identical to those reported in the literature.[20]

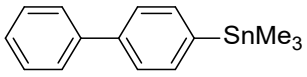

Figure S10: 4-Trimethylstannyl-1,1'-biphenyl

12c-(1,1'-Biphenyl-4-yl)-4,8,12-trioxatriangulene (Fig. 1a) Under nitrogen atmosphere, 4-(trimethylstannyl)-1,1'-biphenyl (103 mg, 324 µmol) was dissolved in dry tetrahydrofurane (5 mL) and cooled to −78 °C. A 1.6 M solution of methyllithium in diethylether (0.20 mL, 324 µmol) was added, and the mixture was stirred for 5 min at −78 °C. Subsequently, a solution of 4,8,12-trioxatriangulenium tetrakis[3,5-bis(trifluoromethyl)-phenyl]-borate (409 mg, 356 µmol) in dry tetrahydro-furane (10 mL) was added dropwise, and the mixture allowed to warm to room temperature where it was stirred for another 18 h. The solvent was then evaporated and the obtained crude product subjected to column chromatography (stationary phase aluminium oxide, eluent dichloromethane/n pentane (1:20, Rf = 0.40)) to yield the analytically pure product as a colourless solid (47.4 mg, 108 µmol, 33 %). For surface preparation, the sample was additionally purified by sublimation (150 °C, 2×10^{-3} mbar, 6 h).

References

(1) Maintz, S.; Deringer, V. L.; Tchougréeff, A. L.; Dronskowski, R. LOBSTER: A tool to extract chemical bonding from plane-wave based DFT. 2016.

(2) Yakutovich, A. V.; Eimre, K.; Schütt, O.; Talirz, L.; Adorf, C. S.; Andersen, C. W.; Ditler, E.; Du, D.; Passerone, D.; Smit, B., et al. AiiDAlab–an ecosystem for developing, executing, and sharing scientific workflows. *Comput. Mater. Sci.* **2021**, *188*, 110165.

(3) Pizzi, G.; Cepellotti, A.; Sabatini, R.; Marzari, N.; Kozinsky, B. AiiDA: automated interactive infrastructure and database for computational science. *Comput. Mater. Sci.* **2016**, *111*, 218–230.

(4) Perdew, J. P.; Burke, K.; Ernzerhof, M. Generalized gradient approximation made simple. *Phys. Rev. Lett.* **1996**, *77*, 3865.

(5) Grimme, S.; Antony, J.; Ehrlich, S.; Krieg, H. A consistent and accurate ab initio parametrization of density functional dispersion correction (DFT-D) for the 94 elements H-Pu. *J. Chem. Phys.* **2010**, *132*, 154104.

(6) Goedecker, S.; Teter, M.; Hutter, J. Separable dual-space Gaussian pseudopotentials. *Phys. Rev. B* **1996**, *54*, 1703.

(7) VandeVondele, J.; Hutter, J. Gaussian basis sets for accurate calculations on molecular systems in gas and condensed phases. *J. Chem. Phys.* **2007**, *127*, 114105.

(8) Tersoff, J.; Hamann, D. R. Theory of the scanning tunneling microscope. *Phys. Rev. B* **1985**, *31*, 805.

(9) Tersoff, J. Method for the calculation of scanning tunneling microscope images and spectra. *Phys. Rev. B* **1989**, *40*, 11990.

(10) Zhang, Y.; Yang, W. Comment on "Generalized gradient approximation made simple". *Phys. Rev. Lett.* **1998**, *80*, 890.

(11) Weigend, F.; Ahlrichs, R. Balanced basis sets of split valence, triple zeta valence and quadruple zeta valence quality for H to Rn: Design and assessment of accuracy. *Phys. Chem. Chem. Phys.* **2005**, *7*, 3297–3305.

(12) Neese, F.; Wennmohs, F.; Becker, U.; Riplinger, C. The ORCA quantum chemistry program package. *J. Chem. Phys.* **2020**, *152*, 224108.

(13) Weigend, F. Accurate Coulomb-fitting basis sets for H to Rn. *Phys. Chem. Chem. Phys.* **2006**, *8*, 1057–1065.

(14) Grimme, S.; Ehrlich, S.; Goerigk, L. Effect of the damping function in dispersion corrected density functional theory. *J. Comput. Chem.* **2011**, *32*, 1456–1465.

(15) Steffen, C.; Thomas, K.; Huniar, U.; Hellweg, A.; Rubner, O.; Schroer, A. TmoleX – a graphical user interface for TURBOMOLE. *J. Comput. Chem.* **2010**, *31*, 2967–2970.

(16) Janowski, T.; Pulay, P. High accuracy benchmark calculations on the benzene dimer potential energy surface. *Chem. Phys. Lett.* **2007**, *447*, 27–32.

(17) Liu, B.; McLean, A. Accurate calculation of the attractive interaction of two ground state helium atoms. *J. Chem. Phys.* **1973**, *59*, 4557–4558.

(18) Jansen, H.; Ros, P. Non-empirical molecular orbital calculations on the protonation of carbon monoxide. *Chem. Phys. Lett.* **1969**, *3*, 140–143.

(19) Van Duijneveldt, F. B.; van Duijneveldt-van de Rijdt, J. G.; van Lenthe, J. H. State of the art in counterpoise theory. *Chem. Rev.* **1994**, *94*, 1873–1885.

(20) Luo, P.; Dinnocenzo, J. P. Mechanism and Unusual Fragmentation Selectivities of Aryltrialkylstannane Cation Radicals. *J. Org. Chem.* **2015**, *80*, 9240–9246.